JOURNAL OF MATERIALS SCIENCE **37** (2002) 3093–3100

High density net shape components by direct laser re-melting of single-phase powders

R. H. MORGAN, A. J. PAPWORTH, C. SUTCLIFFE, P. FOX, W. O'NEILL
Department of Engineering (Manufacturing), The University of Liverpool, Liverpool L69 3GH, UK
E-mail: R.morgan@liverpool.ac.uk

Direct Metal Laser Re-Melting is a variant of the Selective Laser Sintering process, a Rapid Prototyping (RP) technology. This tool-less manufacturing technology has the potential of producing complex, high quality components from single-phase metal powders in short time scales. This is made possible by the production of consecutive two-dimensional layers. Unfortunately, finished components manufactured by this technique have their integrity and material properties dictated by the porosity within the laser re-melted structure. In order to maintain structural integrity comparable to conventionally produced components, metal components produced by the rapid prototyping method should exhibit a porosity of the order of maximum of $\sim$2% with corresponding bulk material properties. To achieve these objectives, process and laser parameters require optimisation for maximum densities to be attained. This paper reports on the development of a scanning strategy that produces stainless steel (316L) laser re-melted components which exhibit porosities of $<$1%, while maintaining the concept of rapid prototyping.

1. Introduction

Rapid Prototyping emerged in the late nineteen eighties as a tool for product designers to produce physical, three-dimensional prototypes of their Computer Aided Design (CAD) models. It allowed prototype production in hours or days rather than the weeks or months typically associated with traditional manual model making processes, thus generating significant time and cost savings.

In general, RP technologies produce 3D solid models by a consecutive layer-wise production of thin (0.1 mm typical) 2D cross sections, each corresponding to a particular slice from the CAD model. The method of layer production is particular to each individual technology; detailed descriptions of which can be seen elsewhere in the literature [1].

Selective Laser Sintering (SLS) is widely regarded as one of the most flexible of RP technologies due to the wide variety of materials, which can be processed, including a range of polymers, elastomers, ceramics and metals [2–5]. Models are produced by selectively scanning a low power (50–100 W) infra-red laser over a powder bed whose temperature has been raised to a value just below the melting point of the powder. The incident power of the laser is then sufficient to selectively melt the powder forming a consolidated layer of the same dimension of the desired cross section of the CAD model. This approach of scanning over a raised temperature bed reduces thermally induced stresses that lead to curling of the layers and helps improve wetting between particles. Any area that does not feature in the 2D slice is not scanned and hence remains unconsolidated acting as a natural support for overhanging features on subsequent layers. Once a layer is complete, a powder delivery device deposits fresh powder over the scanning area and the process repeats with each layer fusing to the previous layer. Upon completion of all the slices, the object is removed from the build chamber and unconsolidated powder is removed.

There are three main process variants of SLS for the production of metallic objects. The first, Indirect Metal Sintering, involves the use of a base metal powder mixed with a polymer binder component. A low energy laser beam selectively fuses the polymer particles, which act as a matrix binding the metal particles together to produce a "green" part. Subsequent furnace processing removes the polymeric constituent through burn out, and fuses the metal powder particles together forming a porous metal component ("brown" part). In order to fill this porosity a lower temperature alloy infiltration stage is required, the resultant part is essentially a 2-component mix of material [6].

Second, Binary Phase Sintering involves the use of a composite powder blend containing two or more alloys. In this instance, the low energy laser beam (50–100 W) fuses the low melt temperature alloy in preference to the high temperature particles, where the low melt component act as a matrix binding the part together [7]. The two processes described above compromise the bulk properties of the resulting component due to the use of inferior alloys and infiltration of porous structures.

The third process route, Direct Metal Sintering, seeks to alleviate some of the problems apparent in current commercial techniques by utilising only single

component powders and striving to achieve 100% density. This process involves the use of a high-energy beam to directly fuse the high temperature powder layer in two-dimensional cross-sections as explained previously.

The problems associated with Direct Metal Laser Sintering are generally due to the high temperatures, involved in the process. Upon illumination of the powder bed, strong surface tension forces act on the melt, driving it towards a minimum surface energy state, which is spherical, leaving areas of porosity between melt tracks [8]. High temperature oxidation of the material, though reduced by inert environment, exacerbates the situation by further reducing wetting between melt beads [9]. High residual stresses are also generated in the layers causing curl and in extreme cases tearing across the layer [10]. The net result of these combined effects is porosity generated in the completed parts. In order to reduce porosity, the effect of pulsed interaction of the incident beam with the powder layer has been investigated with a view to overcoming the forces acting on the melt and effecting a redistribution of the melt by employing a recoil compression force associated with partial vaporisation and plasma formation of the powder substrate [11]. Results showed that, in certain cases, density is improved by the introduction of recoil shock compression [11], however, significant porosity existed in the resulting cubic primitives. Though the recoil force had an effect in increasing density, a maximum density of 89% was achieved with continuous wave (CW) scanning at 100 mm s^{-1}, where little or no plasma was formed. Fig. 1 shows the effect of pulse frequency on the density of cubes (produced by a simple straight line rasterscan) for varying scan speeds and beam overlaps (the amount of overlap between two successive scan lines) in a typical cross section exhibited by the cubes.

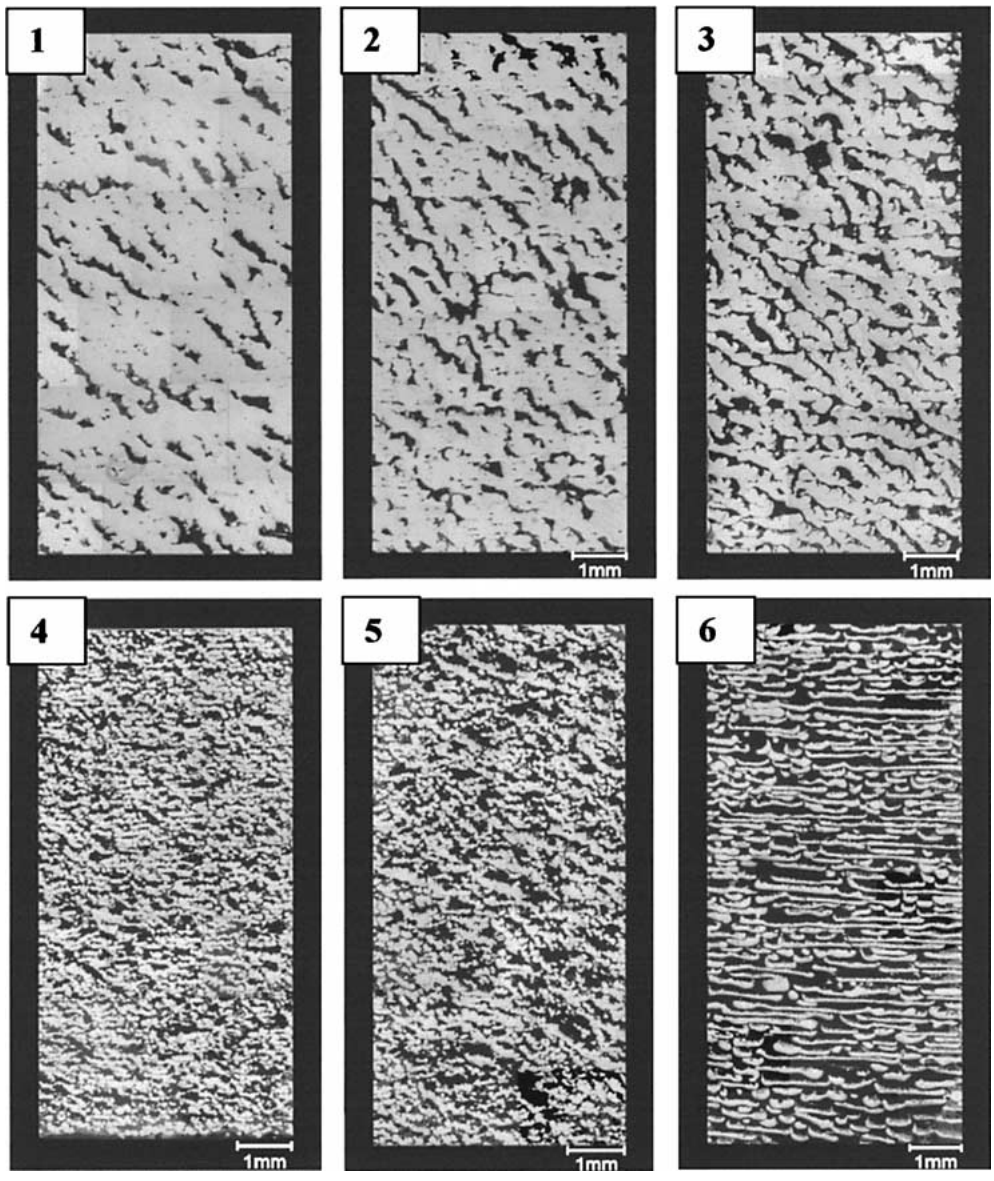

Figure 1 Density analysis of direct laser remelted 316L stainless steel cubic primitives at varying pulse frequencies. Sections are in the plane of laser rasterscan direction. The micrographs show: (1) CW sample at 100 mm/s, 80 W, 25% beam overlap. (2) CW sample at 100 mm/s, 80 W, 50% beam overlap. (3) 60 kHz Pulsed Sample at 100 mm/s, 80 W, 25% beam overlap. (4) 30 kHz pulsed sample at 500 mm/s, 80 W, 25% beam overlap. (5) CW sample at 500 mm/s, 80 W, 25% beam overlap. (6) 10 kHz pulsed sample at 100 mm/s, 80 W, 25% beam overlap. Evidence of pulsed effects is visible in increased density between the Pulsed and CW samples shown in Sections 4 and 5, and also in the detrimental effects of pulsed recoil compression effects visible in the sample shown in Section 6.

Of particular concern in the results was the appearance of a periodic, angular porosity occurring across many layers, visible in Fig. 1 [11].

Previous studies conducted by Morgan *et al.* [11, 12] resulted in optimisation of laser power and scan speed variables for single scan-line walls. The results showed that 100% fully dense 15 mm length walls of height 10 mm could be produced using a 100 μm diameter beam traversing at <80 mm s^{-1}. However, when trying to convert from a single line wall to a cube of material, the porosity within the cube increased to $\sim$20% (Fig. 1). It was also noted that the porosity had a form of structure that followed a wave that could be seen in the surface texture [12]. This paper reports on a scanning strategy, which has been developed to overcome the formation of the wave structure and hence remove the associated porosity within the material in order to achieve full density.

2. Experimental methods

All materials were produced by scanning a Continuous Wave (CW) 100 μm diameter beam with a power rating of 80 W from a Rofin Sinar 90 W Nd : YAG industrial laser marker. Scanning was accomplished by an integrated RSG1014 analogue galvo-scanning head at a scan-speed of 100 mm/s [11, 12]. The beam was directed into an atmospheric controlled experimental test chamber, a schematic of which is shown in Fig. 2. The chamber consists of two computer-controlled platforms, one to control the powder delivery system, the other to control component build parameters. The build and delivery system parameters were optimised for an even 100 μm coating of powder to be layered for every build layer. The powder used was stainless steel 316L, which is a popular welding alloy due to its high corrosion resistance following processing. The powder is spherical, untreated, and is specified as 80% less than 22 μm diameter with a maximum of 60 μm diameter. Samples were prepared for optical metallographic examination by mounting and then grinding using SiC papers to 2500 grit. The samples were then polished to 0.25 μm using diamond paste. The microstructure was then made visible by using an austenite stainless steel etch, which consisted of 40% HCl, 20% HNO_3, balance H_2O. Density analysis was performed on the samples by way of a Xylene impregnation technique [13].

3. Results and discussion

From analysis of the single-line wall builds, which were made with changing scan-speed, it could be seen that the wave structure [12] was independent of speed, until the speed was too fast to create a 100% dense wall. It was also noted that the wave structure shown in Fig. 3a had a periodicity of about 1.5 mm, and had fully developed by the third layer (Fig. 3b). The wave also caused an increase in the wall thickness from 300 μm to 1.5 mm. This increase in thickness is due to two effects;

1. The reduced effect of the conduction properties of the substrate material as the build moves away form the substrate. This reduction in conduction allows heat to build up in the melt resulting in more material being melted from the surrounding powder and hence a wider build;
2. The wave crest being remelted by the next laser pass, which then flowed over the edge of the wall as can be seen in Fig. 3c.

It was also noted that the wave structure was a function of the way in which the wall was made, the structure apparent on the surface of the build was also visible in the microstructure of metallographically prepared samples (Fig. 3d).

It was concluded from this study that the removal of the wave structure in the material is of paramount importance as its formation was responsible for:

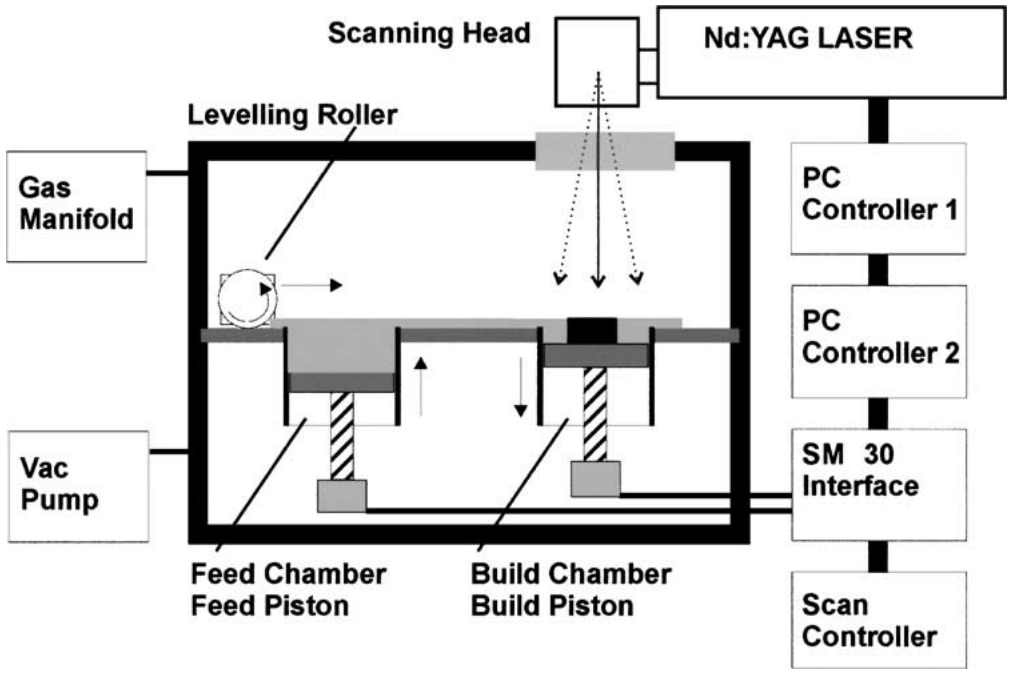

Figure 2 Schematic of Direct Metal Laser Re-Melting experimental test chamber constructed at the University of Liverpool.

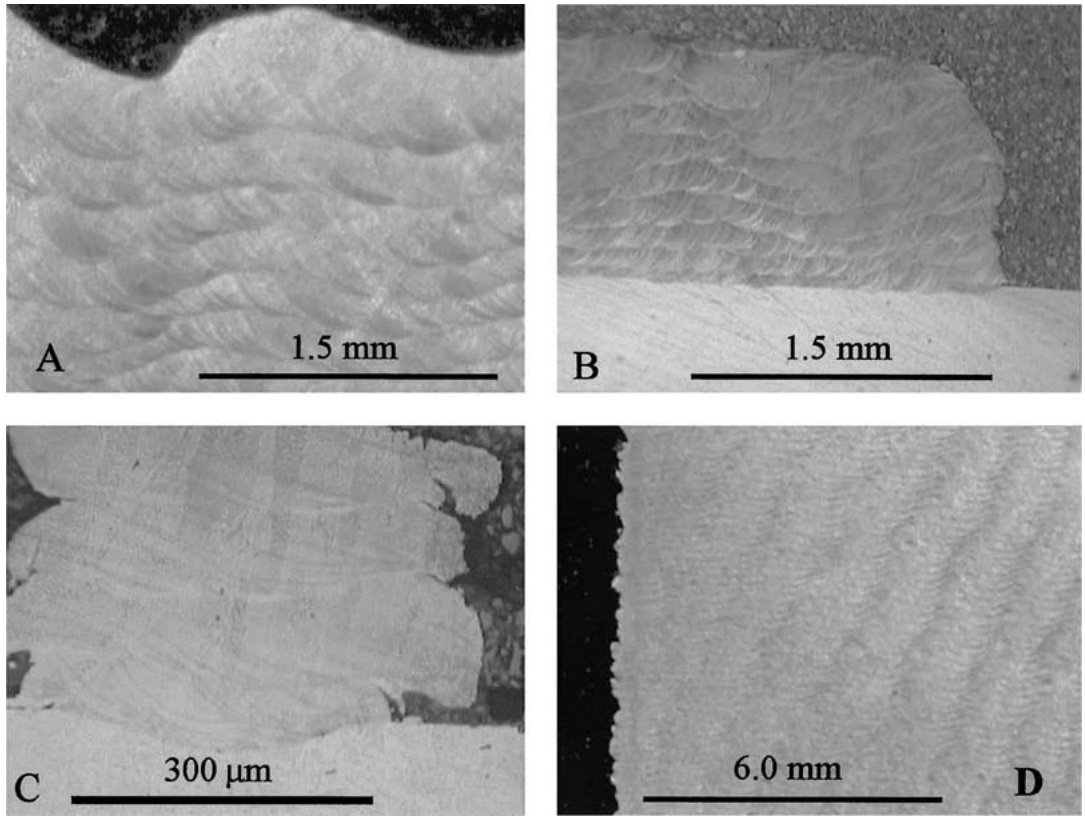

Figure 3 Wave structure shown in (A) has a periodicity of about 1. 5 mm; the wave can be seen to have developed by the fourth layer (B). As the melt pool increases in size it overflows the side of the wall (C) causing the surface roughness. The wave structure was also visible in the microstructure of metallographically prepared samples (D).

1. High surface roughness levels,
2. The porosity seen within the cube of material (Fig. 1).

To investigate the formation of the wave structure, a series of 10 single-line walls of different heights were produced, where the length of scan was fixed at 10 mm (Fig. 4a and b). Each wall was built one layer higher than the previous one to study the evolution of the wave, with respect to layer height. It was determined from the set of 10 walls, that the wave structure was fully developed by the third layer, where upon subsequent layers showed defects in the surface structure as seen in Fig. 4b. Sets of walls were then manufactured to a height of ten layers, each set had a different fixed scan length; these were 5.0 mm (not shown), 2.5 mm (Fig. 4c) and 1.0 mm (Fig. 4d). The 2.5 mm scan length wall showed signs of wave formation, which can be seen as periodic bulging/thickening of the melt track. The wall produced at 1 mm length showed no such formation but a change in surface texture was noted, accompanied a visual reduction in surface roughness. It was concluded that in order to stop the formation of the wave structure, a maximum scan length less than that of the wave period (1.5 mm) should be used in all subsequent operations.

Using this scan length, scan strategies were developed to achieve full or near-full density. Several so-called fill strategies have been assessed in these experiments the results of which are described below. It should be noted here that fill strategies are be divided into 2 groups these are;

1. *Scan strategies*: Base "scan-units" from which an area of a layer is built, they are analogous to the squares of patchwork on a patchwork quilt.
2. *Knit strategies*: The method of joining together scan units to produce the whole layer.

3.1. Scan strategies

The following scanning strategy was adopted, whereby the laser beam was scanned in a bi-directional raster. A single-scan wall, with raster-width of 0.75 mm was chosen to avoid the formation of the wave structure, to produce a 'square-ended' zigzag. The beam overlap between successive rasterscan lines was found experimentally by observing the extent of porosity at their interface. Fig. 5 shows the effect of varying beam overlap between rasterscan lines. In Fig. 5a, a 50% overlap causes regions of porosity between consecutive scan lines. As the overlap is decreased, as shown in Fig. 5b–d, the resulting density increases, optimised in a −15% overlap, i.e., a gap between scan lines.

At 50% beam overlap, there is a significant increase in thermal energy imparted to the powder bed. This results in a large increase in the volume of the melt bead, as the local surrounding powder is drawn into the melt volume through the increased radial conductivity into the powder layer. On the subsequent pass, the beam scans 50% of the previous melt bead while the remainder finds the local area devoid of powder and consequently scans an empty space, thus leading to areas of porosity. Therefore, the size of the melt bead (due to the conduction effects) compared with the beam diameter explains the successful production of full density walls

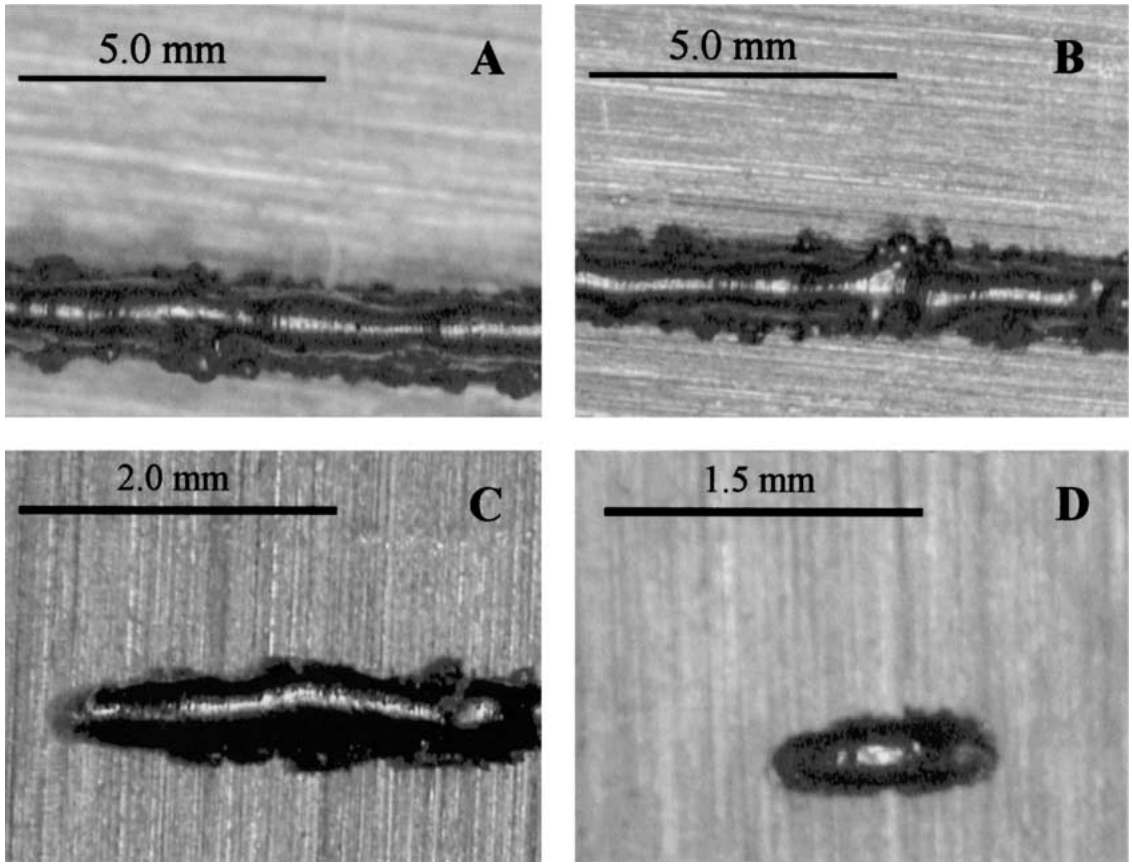

Figure 4 Single-line walls were constructed at different heights to assess the effect of wave formation on the surface roughness as build height is increased (a and b). Wave formation is still apparent through evidence of rough wall surfaces with reduction of scan length to 2.5 mm (c). Smooth sided walls can be produced when scan length is less than that of the wave period (1.5 mm) shown in (d).

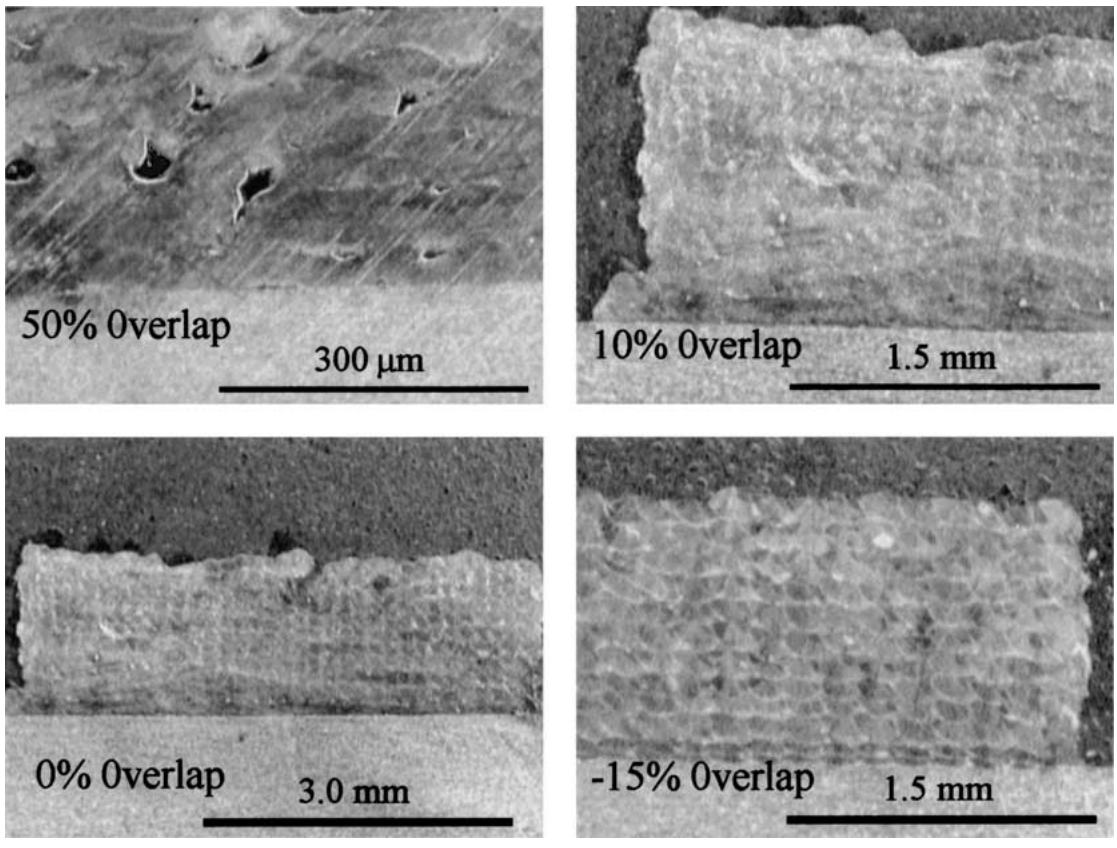

Figure 5 Section views of melt beads produced by a bi-directional rasterscan strategy. 50% overlap between neighbouring melt beads creates regions of porosity at the interface. As overlap is reduced, porosity is minimised and eliminated when a negative overlap is applied to the scan strategy.

with decreasing overlap, as neighbouring melt beads fuse together. The most efficient use of the powder bed was obtained with the use of a negative 15% overlap, where the section of each melt bead can be clearly seen, as shown in Fig. 5d.

The bi-directional rasterscan with negative beam overlap between neighbouring scan lines makes up the scan unit for the Scanning Strategy (Fig. 6a). The following section describes the work undertaken to knit the scan units together to successfully produce a full or near-full density layer.

3.2. Knit strategies

3.2.1. Strategy 1: ordered knitting

Experiments were undertaken to investigate how the scan-units could be joined together to form a 100% dense layer. Initial work examined the variation of overlap between two consecutive scan units. The overlap varied from 75% to 10% of the raster-width (0.75 mm). It was found that full density could be achieved across the two scan units with a 15% overlap, however the addition of further scan units caused regions of porosity across the interfaces. The reason was attributed to the conduction effects increasing melt pool volume, thus drawing in loose powder from each of the sides of the scan-unit.

3.2.2. Strategy 2: odd-even knitting

To attempt to overcome the melt pool drawing powder as described above, a knitting strategy shown in Fig. 6b was undertaken, where scan-units were laid down in an odd-even manner, such that scan-units

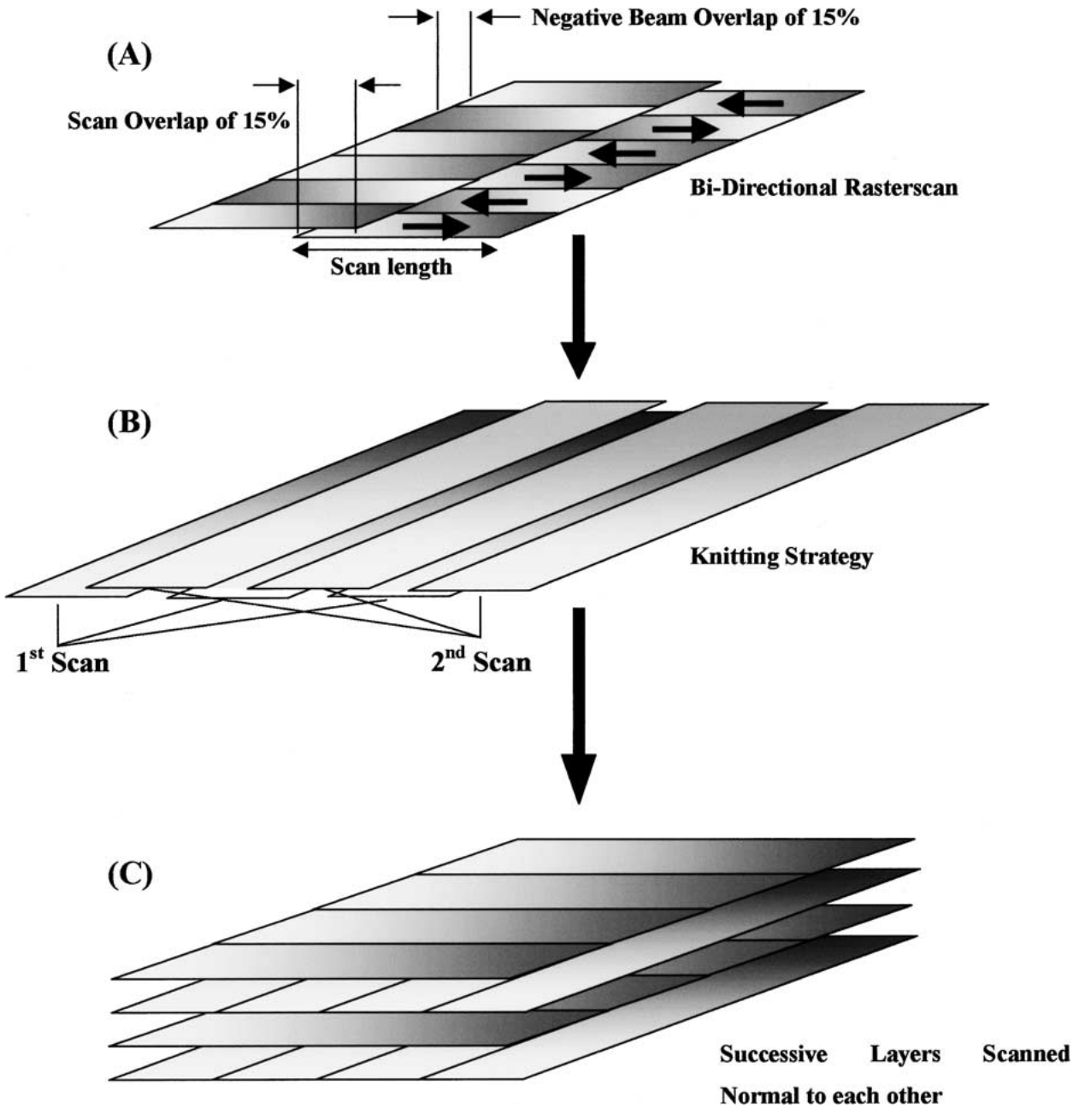

Figure 6 Schematic of the scan-unit strategy developed to produce ~99% dense material. Schematic (A) shows the bi-directional rasterscan strategy with changing beam direction and beam overlap, schematic (B) shows the knitting strategy of the scan-units, and (C) how layers are scanned normal to each other to reduce porosity.

1, 3, 5. . . (Fig. 6b—1st scan) were first scanned with a separation of 70% of the rasterscan length between them. The 70% value was determined from the previous experiments of scan-unit overlaps, where 15% overlap was optimum. Before the even scan-units were scanned, a powder re-fill sequence was introduced to replace powder lost on either side of the scanned areas. Powder was deposited over the powder bed without any change in build height, thus maintaining the correct position in the z-axis. Upon completion of the powder re-fill, the even scan-units 2, 4, 6. . . (Fig. 5b—2nd scan) were scanned. Densities of ∼95% were recorded by this knit strategy.

3.2.3. Strategy 3: odd-even knitting, normal consecutive layers

In strategy 2, it was noted that pores were always in the same location between each successive layer. In order to investigate the cause of these defects, four samples were produced, each sample increasing in height by a single layer. Analysis of the surfaces showed once a pore had formed, its presence would propagate through subsequent layers forming an interconnected void. To eliminate the occurrence of this porosity, consecutive layers were scanned normal to each other as shown in the schematic Fig. 6c. This resulted in the production of a material that was ∼98% dense with occasional pores still apparent between layers. It is postulated here that the origin of the remaining pores was gas entrapment between layers. The mechanism for this is as follows; a rough surface causes the entrapment of gas upon deposition of a new powder layer. During the scanning of the new layer, the gas is superheated and expands rapidly removing the liquid metal above it, thus creating a large pore.

3.2.4. Strategy 4: cleaned, odd-even knitting, normal consecutive layers

To overcome the problem of gas entrapment, the surface of the build layer was smoothed by a third laser process, which was added to the knitting strategy of each layer. The purpose of this third process step was to re-melt the surface releasing any entrapped gas and to create a smooth surface finish to each layer (Fig. 7). Although the surface shown in Fig. 7 looks rough, the higher magnification micrograph (insert A) shows that the surface of the build is flat. The smoothing scan consisted of a larger bi-directional rasterscan of width 1.5 mm maintaining the beam overlap at −15% and knit overlap of 15%.

This multi layer quilting strategy utilising scan-units and smoothing scans, as shown in the schematics of Fig. 6, produced cubes of material that were consistently over 99% dense, as shown in Fig. 8.

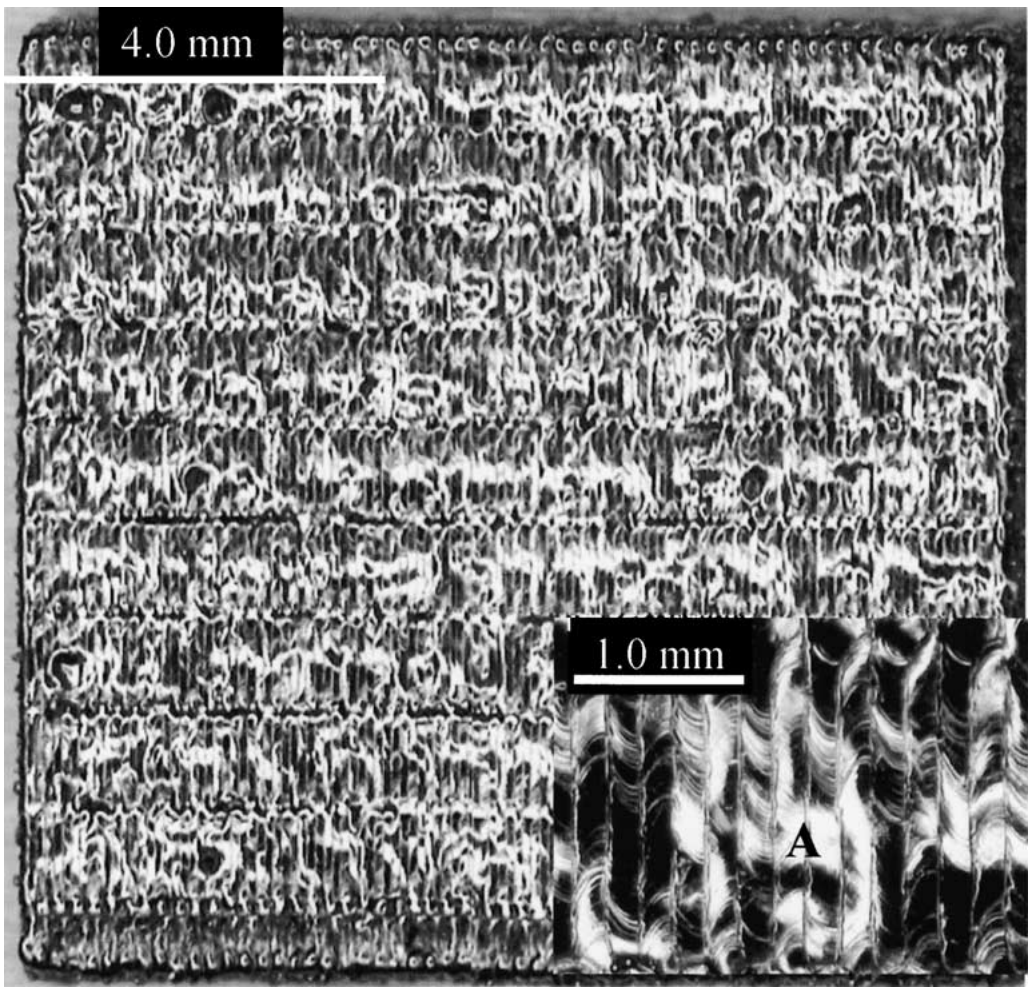

Figure 7 The (1.5 mm scan-unit) smoothing scan removes gas entrapment and prepares the surface for the next layer. The insert (A) shows just how smooth the prepared surface is.

Figure 8 Polished cube of 316L stainless steel material. Density measured at >99. 5%.

4. Conclusions

1. The cause of the surface roughness and the porosity within a cube of material was due to the formation of a wave structure in the solidified material, as evidenced by its existence during the production of single scan-line walls. The wave structure had a periodicity of 1.5 mm and had fully developed by the third layer of the build.

2. The adoption of a bi-directional rasterscan strategy was developed for the removal of the periodic wave structure by reducing the raster-width to less than that of the wave period. By this method, 100% density 0.75 mm thick walls were produced.

3. Interfaces between neighbouring walls were shown to exhibit porosity. A further scanning strategy was developed which incorporated a powder redeposition stage within the production of a single layer, in order to remove the occurrence of the interfacial porosity. A further development of the scanning strategy was the addition of a laser surface clean stage to smooth surface roughness and remove any possible gas entrapment.

4. Consecutive layers were scanned normal to each other to avoid the formation of interconnected porosity. The scanning strategy produced cubes of material, which were repeatable and had a porosity of less than 1%.

Acknowledgements

The authors would like to thank Mr Lawrence Bailey for his invaluable contribution to the continuous development of the research equipment. We would also like to thank the EPSRC for their support of the program through a ROPA award.

References

1. J. P. KRUTH, M. C. LU and T. MAKAGAWA, *CIRP Annals, Mfg. Tech.* **47**(2) (1998) 525.
2. C. K. CHUA, S. M. CHOU and T. S. WONG, *Int. J. Adv. Manuf. Tech.* **14** (1998) 146.
3. I. GIBSON and D. SHI, *Rapid Prototyping J.* **3**(4) (1997) 129.
4. C. NELSON, N. K. VAIL, J. W. BARLOW, J. J. BEAMAN, D. L. BOURELL and H. L. MARCUS, *Ind. Eng. Chem. Res.* **34** (1995) 1641.
5. D. L. BOURELL, H. L. MARCUS, J. W. BARLOW and J. J. BEAMAN, *Int. Journ. Powder Metallurgy* **28**(4) (1992) 369.
6. C. NELSON, Rapid steel 2.0 mold inserts for plastic injection molding, DTM Corporation, www.dtm-corp.com (1998).
7. J. P. KRUTH, B. VAN DER SCHUEREN, J. E. BONSE and B. MORREN, *CIRP Annals* **45**(1) (1996) 183.
8. W. MEINERS, K. WISSENBACH and R. PROPAWE, in Laser Assisted Net Shape Engineering 2, Proc. LANE (1997) p. 615.
9. C. HAUSER, T. H. C. CHILDS, K. W. DALGARNO and R. B. EANE, in Proc. Solid Freeform Fabrication Symposium, (1999) Vol. 10, p. 265.
10. R. MORGAN, C. J. SUTCLIFFE and W. O'NEILL, *Rapid Prototyping J.* **7**(3) (2001) 159.
11. *Idem.*, *Optics and Laser in Engineering*, submitted.
12. R. MORGAN, A. PAPWORTH, C. SUTCLIFFE, P. FOX and W. O'NEILL, in Proc. Solid Freeform Fabrication Symposium 2001, Accepted.
13. G. ARTHUR, *J. Inst. Mat.* **83** (1954) 329.

Received 3 June
and accepted 15 December 2001